GEOQuébec 2015
Challenges from North to South
Des défis du Nord au Sud

InSAR Monitoring of Transportation Infrastructure in Permafrost Regions

J. Eppler, M. Kubanski, J. Sharma and J. Busler
MDA Systems Ltd., Richmond, British Columbia, Canada
J. Roger and M. Allard
Centre d’Etudes Nordiques, Université Laval, Québec, Canada

ABSTRACT

The combined effect of climate change and accelerated economic development in Northern regions increases the threat of permafrost related surface deformation of transportation infrastructure. Satellite based Synthetic Aperture Radar Interferometry (InSAR) provides a means for monitoring deformation over remote and spatially extensive areas and is hence potentially well suited for monitoring Northern roadways.

However, permafrost poses challenges for InSAR monitoring due to complex deformation patterns caused by seasonal heave and settlement of the active layer with freeze-thaw cycles. We have developed an InSAR method that optimizes spatial and temporal resolution by joint adaptive filtering of multiple InSAR datasets.

The proposed InSAR method is demonstrated using data collected over the communities of Salluit and Umiujaq in Northern Quebec. Surface deformation estimates are compared to surficial geology maps provided by project partners from the Centre d'Études Nordiques and show potential for mapping risks to infrastructure posed by permafrost.

RÉSUMÉ

L’effet combiné du changement climatique et de l’accélération du développement économique dans les régions nordiques augmente les risques de déformation des infrastructures de transport liés à la dégradation du pergélisol. L’acquisition de données satellites par Synthetic Aperture Radar Interferometry (InSAR) s’avère un outil efficace de surveillance des déformations en région éloignée et ce, à grande échelle permettant un suivi efficace des infrastructures de transport en milieu nordique.

Toutefois, la présence de pergélisol s’avère un défi pour le suivi des déformations à partir de la technologie InSAR en raison des patrons de déformation complexes causés par le soulèvement et le tassement de la couche active dus aux cycles de gel et dégel. Une méthode basée sur la technologie InSAR permet d’optimiser la résolution spatiale et temporelle à partir de la mise en commun d’un filtrage adaptif à plusieurs séries de données InSAR.

La méthode InSAR proposée dans cet article est basée sur des données provenant des villages de Salluit et d’Umiujaq au Nunavik. La surface de déformation estimée pour ces villages est comparée à des données in situ fournies par le Centre d’études nordiques (CEN), partenaire dans ce projet. Les données obtenues permettent d’évaluer et de cartographier les zones à risques d’aménagement en milieu à pergélisol.

1 INTRODUCTION

Permafrost areas pose challenges for existing and planned infrastructure because of the potential surface deformation induced by either long-term changes to the permafrost state or seasonal active layer fluctuations. Synthetic Aperture Radar Interferometry (InSAR) provides a means to remotely and repeatedly measure over wide areas the surface deformation which may result from these effects (Massonnet et al. 1993).

Permafrost related surface deformation may be temporally complex due to a combination of seasonal heave and settlement of the active layer with freeze-thaw cycles, long term deformation and non-linear or sudden onset deformation related to slope failures. This poses a challenge for space-borne SAR monitoring which is limited by the orbital repeat interval of the satellite. Data derived from a single orbital track may not sufficiently sample the time varying deformation signal. In addition, the surface deformation can be spatially complex due to local variations in ground ice content and surficial geology. This poses an additional challenge for InSAR based methods which typically rely on assumptions of spatial signal continuity to resolve ambiguities in the measurement data. For these reasons an InSAR solution for permafrost monitoring should provide a means for achieving deformation estimates with sufficiently high spatial and temporal resolution.

This paper presents a multiple stack InSAR method for monitoring infrastructure in permafrost regions that involves jointly processing image stacks from multiple view geometries. Combining multiple time series image sets (data stacks) overcomes the temporal sampling limit posed by the satellite orbit cycle. The proposed method also addresses the need for finer spatial resolution by employing spatially adaptive multi-looking over local homogenous neighborhoods to optimize the spatial density of monitored targets (Parizzi and Brcic 2011).

We demonstrate the proposed method for two cases: 1) monitoring the community of Umiujaq, Quebec and the surrounding area with a set of three RADARSAT-2 data stacks over a 21 month period and 2) monitoring the community of Salluit, Quebec with two TerraSAR-X data stacks over a 15 month period. Both Umiujaq and Salluit are remote but growing coastal communities in areas of Northern Quebec with infrastructure that is sensitive to permafrost changes (Allard et al. 2012). Deformation estimates for the two studied cases are decomposed into estimates of long-term linear deformation and seasonal active-layer deformation magnitude and compared to high resolution surficial geology maps. Fortier et al. (2012) report InSAR derived long term subsidence and seasonal deformation estimated over Salluit using ERS-1 and ERS-2 data from 1992-2000.

The proposed multiple stack InSAR method (termed Multi-Track Homogenous Distributed Scatterer (HDS) InSAR) is introduced in Section 2 along with a description of temporal component modelling for separating long term and seasonal deformation components. Section 3 provides details of the test sites and associated data used in the study. Section 4 presents the deformation estimates for the two study cases and compares them to mapped surficial geology. Conclusions of the study are provided in Section 5.

2 METHOD

2.1 Multiple Stack InSAR Technique

The temporal sampling rate of single-stack InSAR surface deformation estimation is limited by the satellite or constellation orbit track repeat rate. One obvious method for increasing temporal sampling is to process multiple stacks from same side satellite view geometries and interleave the results a posteriori. However it is better to jointly process the stacks together because: 1) processing of short stacks (<15 scenes) may lead to significantly degraded results and 2) even if each stack can be successfully processed alone, the intermediate processing steps will not benefit from all available joint information. There are several steps in the HDS-InSAR (Rabus et al. 2012) processing sequence that benefit from a higher temporal sampling. By processing the stacks jointly, these benefits may be realized throughout the processing sequence and not just in the final result. Figure 1 shows the Multi-Track HDS-InSAR processing chain and highlights the steps that benefit from joint processing.

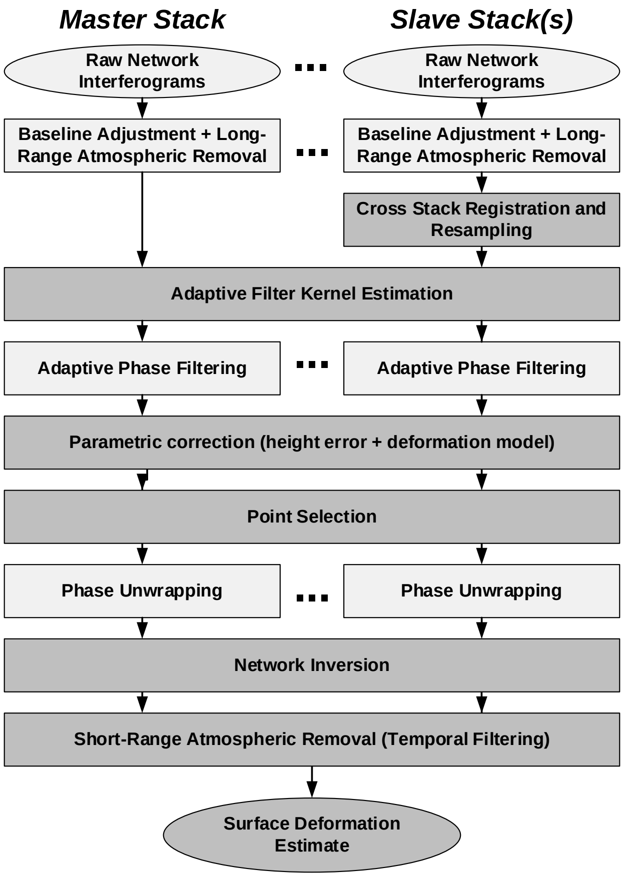

Figure 1. Multi-Track HDS-InSAR processing flowchart. Dark boxes correspond to joint processing steps.

2.2 Temporal Component Modelling

A linear temporal component model was implemented in order to separate seasonal deformation from long-term deformation trends. The implemented model incorporates two components: 1) a seasonal deformation component consisting of a linearly scaled template derived from the ambient mean daily air temperature history and 2) a long term temporally linear component.

Seasonal deformation due to the annual freeze/thaw cycle of the active layer can be modelled using the Stefan's equation and available temperature history data as described in (Liu et al. 2012). In this case simplifying assumptions include symmetric behaviour between the freeze and thaw periods and vertically uniform soil properties and ice concentration. Figure 2 shows an example of multi-season air temperature history and the derived seasonal deformation template.

This model is then used both during parametric phase correction to reduced spatial phase gradients prior to phase unwrapping and then to linearly decompose the final surface deformation estimate into long term linear and seasonal deformation components.

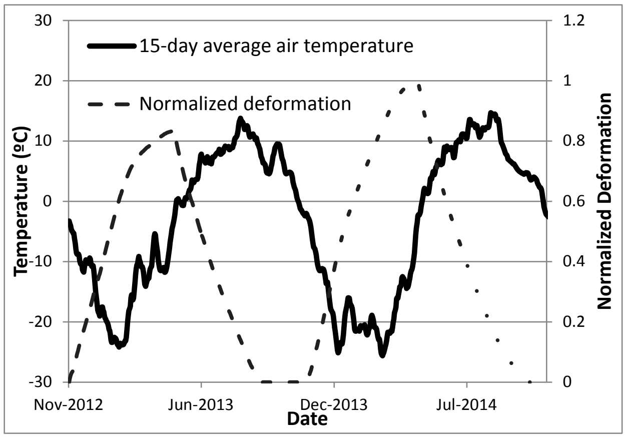

Figure 2. 15-day average air temperature history (source data Environment Canada, http://climate.weather.gc.ca/ accessed November 27, 2014.) and derived active layer deformation template for Umiujaq.

3 STUDY DATA

3.1 Umiujaq, Quebec

Umiujaq (56.6°N, 76.5°W) is a remote community on the eastern coast of Hudson Bay with a population of approximately 450 people. Infrastructure includes buildings within the town site, an airport south of the town and an airport access road. Umiujaq is located in the sporadic permafrost zone, situated at the northern limit of the treeline and the southern limit of discontinuous permafrost (May et al. 2011). May (2011) provides a summary of Umiujaq vegetation and climate conditions. The vegetation is typical of subarctic forest tundra with dwarf shrubs, sedges, grasses and mosses interspersed with patches of trees up to 2 m in height. The mean annual air temperature from 1971 to 2000 was -5.4°C. Umiujaq displays a high seasonal variability due to its proximity to Hudson Bay. From June to December the climate is maritime with moderate temperatures, but after freezing of Hudson Bay the climate becomes more continental and very cold. The area has numerous ice-rich periglacial features, such as palsas and lithalsas, created by frost heaving (Fortier et al. 2008).

Three RADARSAT-2 Spotlight mode stacks covering Umiujaq and surrounding areas were acquired over a 21 month period including two snow free summer seasons in 2013 and 2014. Table 1 summarizes the characteristics of this dataset. Figure 3 shows the spatial footprints of the three stacks and the area processed for this study.

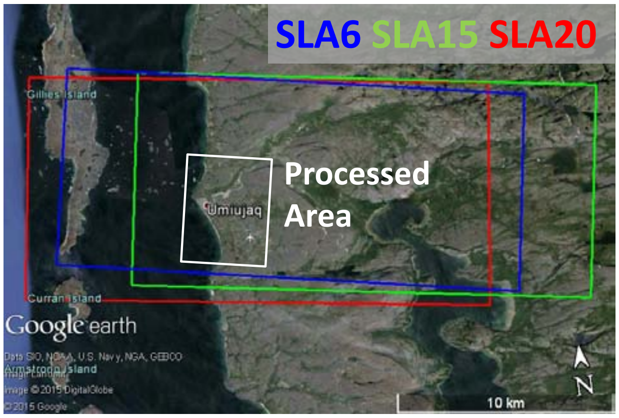

Figure 3. RADARSAT-2 Spotlight mode stack footprints for the Umiujaq, Quebec study site.

3.2 Salluit, Quebec

Salluit (62.2°N, 75.6°W) is the second northernmost Inuit community in Quebec. The town borders the Hudson Strait and has a population of roughly 1360 residents and growing, increasing the demand for housing, commercial, and institutional buildings as well as roads and other municipal infrastructure (Allard et al. 2010). The town is not accessible by road, only by air through Salluit Airport.

The main portion of the village is built in a valley surrounded by steep slopes. Salluit is located in the continuous permafrost zone with many areas of the village containing ice-rich permafrost. The steep slopes and ice-rich permafrost put the village at risk for avalanches, landslides, and permafrost erosion. The warming climate adds further risk of thaw settlement and slope instability in the area, which has experienced a mean annual temperature increase of 2°C since the 1961-1990 reference period (Fortier et al. 2012). The topography surrounding Salluit is hilly and the vegetation is observed to be primarily tundra.

Two TerraSAR-X stacks covering Salluit and surrounding area were acquired over a 15 month period including a single snow free season in 2014. Table 2 summarizes the characteristics of this dataset of 55 images. Figure 4 shows the spatial footprints of the two stacks and the area processed for this study.

Table 1. Summary of RADARSAT-2 (RS-2) stacks for Umiujaq study site.

Sensor	Beam	Pass	Incidence Angle [°]	Ground res [m]	Azimuth res [m]	Swath [km]	Scenes	Start/End dates
RS-2	SLA6	Des	34.7	2.8	0.8	18x8	16	2013/08/14 – 2014/09/02
RS-2	SLA15	Des	41.4	2.4	0.8	18x8	22	2013/01/24 – 2014/10/10
RS-2	SLA20	Des	44.8	2.3	0.8	18x8	19	2013/08/07 – 2014/10/13

Table 2. Summary of TerraSAR-X (TSX) stacks for Salluit study site.

Sensor	Beam	Pass	Incidence Angle [°]	Ground res [m]	Azimuth res [m]	Swath [km]	Scenes	Start/End dates
TSX	HS39	Des	34.7	1.1	1.1	5x5	28	2013/12/27 – 2015/03/12
TSX	ST17	Des	24.6	1.4	0.2	4x4	27	2014/01/02 – 2015/03/29

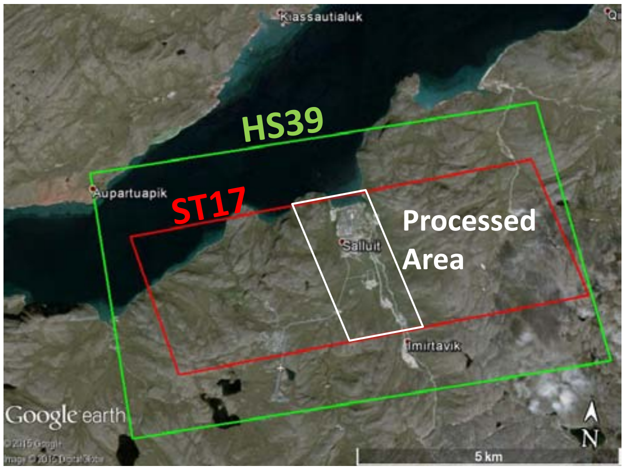

Figure 4. TerraSAR-X spotlight mode stack footprints for the Salluit, Quebec study site.

4 RESULTS

For each of the two study sites all data stacks were jointly processed to derive surface deformation estimates. These line-of-sight estimates were then projected to the vertical direction according to the SAR acquisition geometry. This results in a surface deformation time series estimate for each coherence target in the processed area. For each of these targets the deformation time series data were used to estimate both a linear deformation rate and a seasonal deformation magnitude. These per-target parameters were then rendered spatially to form both linear and seasonal deformation component maps for each study site area.

4.1 Umiujaq, Quebec

Deformation component maps for the Umiujaq site are shown in Figure 5 along with a surficial geology map provided by Centre d'Etudes Nordiques, Université Laval. The top row shows results for Umiujaq and the surrounding area including the airport to the south east of the town site and the connecting access road. The bottom row shows an inset of the town site only.

The deformation component maps render the subset of spatial points which exceed a minimum temporal coherence threshold. Low coherence targets exhibiting high phase noise are eliminated from the processing and not shown on the maps. A comparison of the spatial distribution of coherent targets with the surficial geology shows that areas of surface rock have a high spatial density of coherent targets (nearly continuous), areas of eolian and glaciofluvial sediments have a medium density and areas of current beach, littoral marine sediments and undifferentiated alluvial sediments are only sparsely covered by coherent targets. Infrastructure such as buildings, road surfaces and the airport runway correspond to high coherent target densities. The roads in the area are primarily asphalt surfaced while the airport runway is surfaced with crushed stone (0 - 20mm).

The linear deformation map is rendered with a color scale that shows stable areas as green, subsidence as yellow/red and uplift as cyan/blue. Although most of the processed area shows little or no linear deformation there are some notable areas showing subsidence exceeding 0.5 cm/yr. These include an isolated patch of subsidence in the main town site corresponding to a residential building, several patches in the area of new construction immediately south of the main town site and also the south river bank immediately north of the main town site. Figure 6A shows an example deformation time series from the noted linear subsidence patch within the town site. Although this patch is relatively small and not likely of great significant it is noteworthy because it is distinct from the rest of the town site and the cause of the deformation was not apparent from a visual inspection of the site.

The seasonal deformation maps are rendered with a color scale that extends from dark blue corresponding to zero seasonal deformation to red corresponding to 2 cm of peak-to-peak seasonal deformation. Most areas including nearly all surficial rock areas correspond to minimal seasonal deformation. However there are several glaciofluvial areas showing high seasonal amplitudes. It is noteworthy that the airport runway shows higher seasonal amplitude than the surrounding areas. Within the inset map a section of the road shows higher seasonal amplitude than the rest of the road. An example time series from this road section is shown in Figure 6B. This shows a typical heave and settlement pattern associated with freezing and thawing of the ice-poor active layer beneath the road bed.

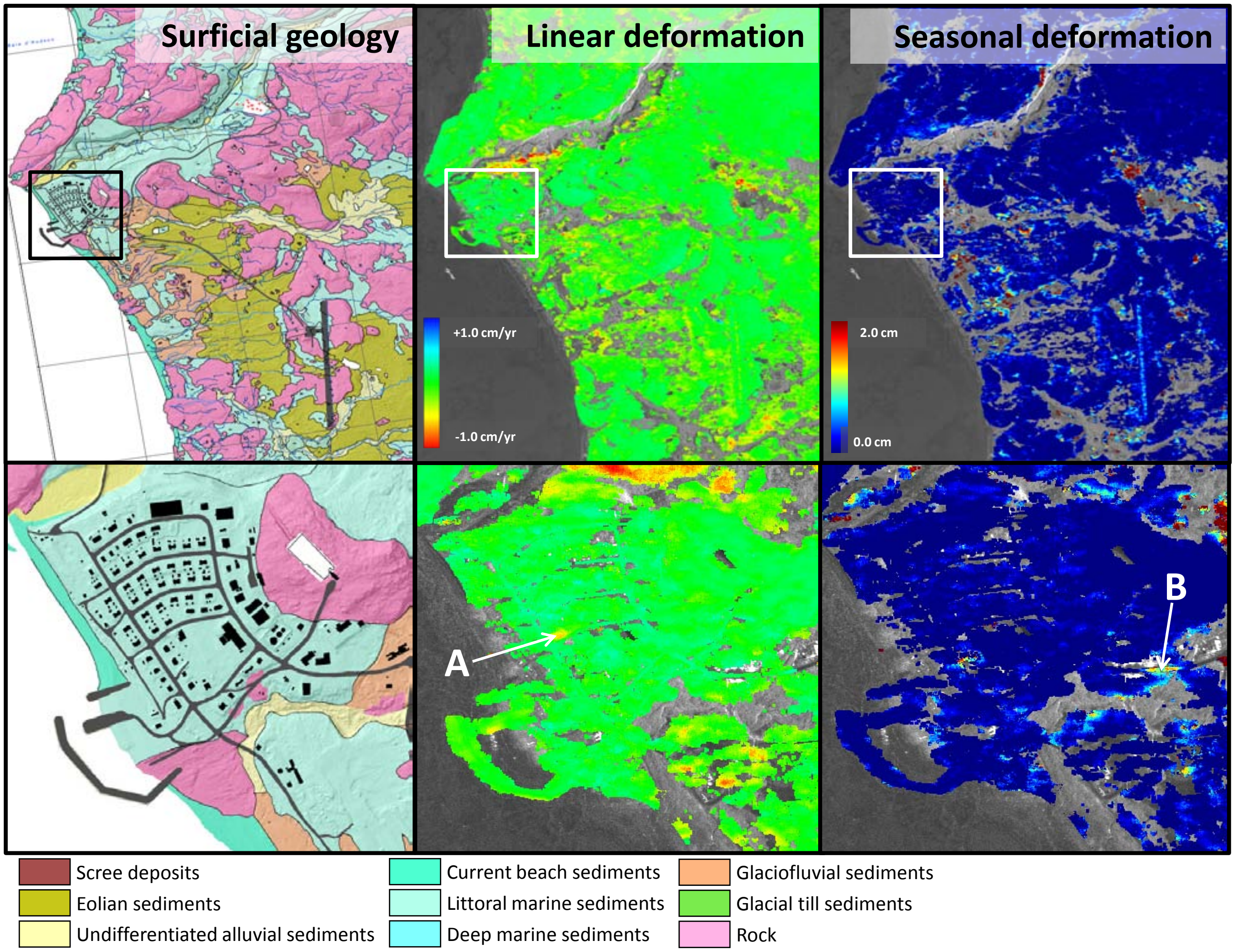

RADARSAT-2 Data and Products © MacDonald, Dettwiler and Associates Ltd (2012-2015). All Rights Reserved. RADARSAT is an official mark of the Canadian Space Agency.

Figure 5. InSAR derived surface deformation estimates (from RADARSAT-2) and surficial geology maps for Umiujaq and surrounding area (top row) and inset of Umiujaq village site (bottom row). Points of interest: A) linear subsidence in town site, B) section of road with seasonal deformation.

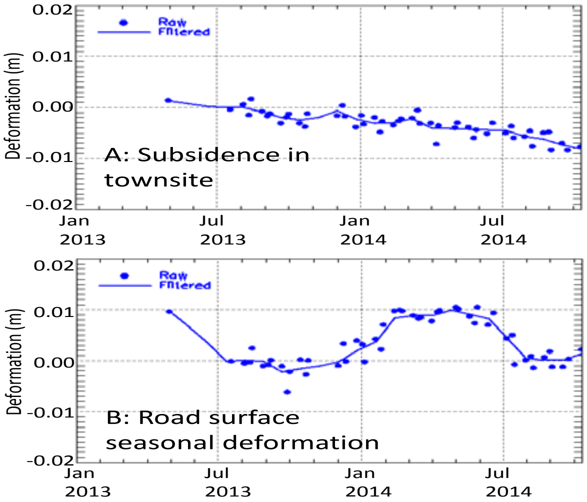

Figure 6.Vertical deformation time series for two points in Umiujaq inset area.

4.2 Salluit, Quebec

Deformation component maps for the Salluit site are shown in Figure 7 along with a surficial geology map of the area provided by Centre d'Etudes Nordiques. These results show high coherent target density in the mapped surficial rock areas and lower target densities in other areas. The road surfaces correspond to low coherent target densities which contrasts that observed for the Umiujaq area roads. Streets in the village are paved on very thin embankments and are laid over frost sensitive clay. The road to the airport, south of town, was rebuilt in summer 2012 has a 2m high embankment and its surfaced is finished with a crush stone layer (0 - 20mm).

The Salluit deformation component maps appear less spatially smooth than the Umiujaq maps which may be due to seasonal effects in the dataset. The Salluit dataset is composed of a single snow free season (summer 2014) bracketed by two snow seasons whereas the Umiujaq dataset is composed of two full snow free seasons bracketing a single snow season. The phase quality of snow season interferograms is expected to be lower than for those that are snow-free due to a combinations of decorrelation effects and snow induced phase bias (Short et al. 2011). The time series of the Salluit coherent targets are therefore bracketed by temporal segments of higher phase noise which may significantly reduce the accuracy of the fitted parameters.

Both the linear and the seasonal deformations occur in the cover of surficial sediments which consist of ice rich marine clay on the valley floor and ice rich thick till on the slopes and on the surrounding plateaus. Buildings in the densely built urban area move up and down a few centimeters with every freeze-thaw cycle of the active layer. Abundant gelifluction in till on the slopes (thin till over bedrock) also displaces the terrain surface (speckled yellow and red dots over the green zone on the linear deformation map.

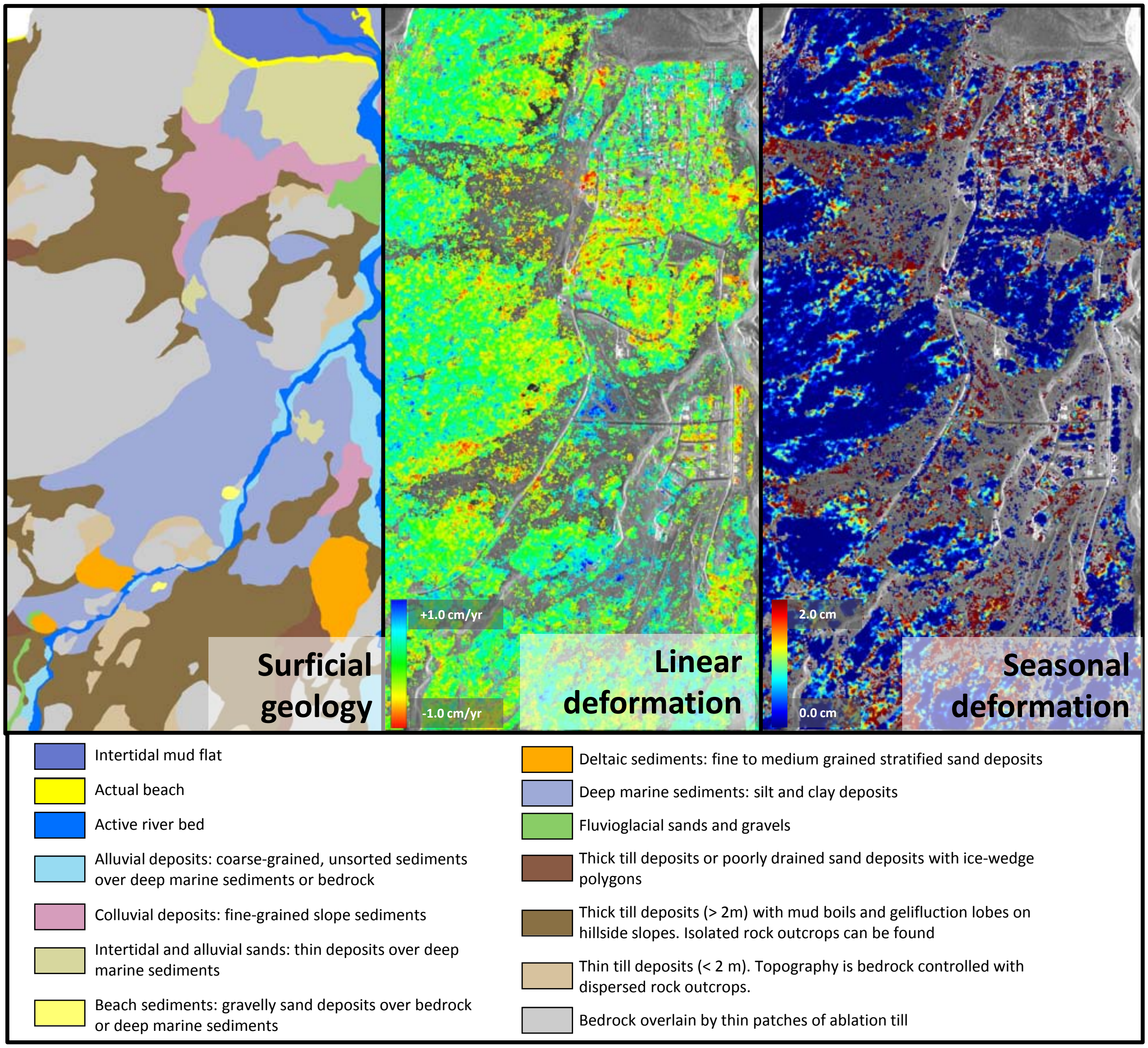

Figure 7. InSAR derived surface deformation parameter maps (from TerraSAR-X) and surficial geology for Salluit and surrounding area.

5 CONCLUSIONS

This study presents an InSAR method for monitoring infrastructure in permafrost areas which involved jointly processing multiple SAR data stacks to achieve a higher temporal resolution than could be achieved with an individual stack. Additionally the method employs spatially adaptive multi-looking to preserve spatial resolution while supressing phase noise in distributed targets. These in combination provide a means for estimating surface deformation with higher spatio-temporal resolution than may be achieved with many existing methods.

The good spatial correspondence between measured unstable areas and surficial geology reflects the distribution pattern of frost sensitive soils and soils that are affected by slope movements. This is particularly evident in Salluit. In Umiujaq deforming areas are more difficult to explain only by active layer shifts; however it is known that bodies of ice-rich silt occur underneath the thick raise shoreline marine sand cover. In these areas permafrost thawing is occurring at greater depth.

ACKNOWLEDGEMENTS

Funding for this work and RADARSAT-2 imagery has been provided by CSA through the Earth Observation Application Development Program (project 9F043-12063/002/MTB). TerraSAR-X data has been provided by the DLR (proposals LAN2045 and LAN2358).

Surficial geology maps for the study sites were provided by Centre d’Etudes Nordiques at Université Laval.

REFERENCES

Allard, M., Lemay, M., Barrette, C., L'Hérault, E., Sarrazin, D., Bell, T. and Doré, G. 2012, Permafrost and climate change in Nunavik and Nunatsiavut: importance for municipal and transportation infrastructures., *From science to policy. An integrated impact study (IRIS) of climate change and modernization*, 171-197.

Allard, M., L'Hérault, E., Gibéryen, T., and Barrette, C. 2010. L'impact des changements climatiques sur la problématique de la fonte du pergélisol au village de Salluit, Nunavik. *Rapport final: Salluit: s'adapter et croître*. Technical report, Centre d'études nordiques, Université Laval.

Fortier, R., LeBlanc, A. M., Allard, M., Buteau, S., and Calmels, F. 2008. Internal structure and conditions of permafrost mounds at Umiujaq in Nunavik, Canada, inferred from field investigation and electrical resistivity tomography. *Can. J. Earth Sciences*, 45:367-387.

Fortier, R., LeBlanc, A.-M., Falorni, G. and R. Therrien, 2012. PSInSAR monitoring of ground movement at Salluit, Quebec (Canada), due to freeze-thaw cycles, active layer thickening, and permafrost warming. Proceedings, Tenth International Conference on Permafrost, Salekhard, Autonomous District of Yamal-Nenets, Russia, Vol. 1, International Contributions, pp. 113-118.

Liu, L., Schaefer, K., Zhang, T., and Wahr, J., 2012. Estimating 1992–2000 average active layer thickness on the Alaskan North Slope from remotely sensed surface subsidence. *Journal of Geophysical Research*: Earth Surface (2003–2012), 117(F1).

Massonnet, D., Rossi. M., Carmona. C., Adragna, F., Peltzer, G., Feigl, K., and Rabaute, T., 1993. The displacement field of the Landers earthquake mapped by radar interferometry, *Nature*, 364(6433), 138-142.

May, I. 2011. *Using in-field and remote sensing data to monitor permafrost dynamics in Northern Quebec*. PhD thesis, Fakultät für Geowissenschaften der Ludwig-Maximilians-Universität München.

May, I., Ludwig, R., and Bernier, M. 2011. Using TerraSAR-X imagery for the monitoring of permafrost dynamics in Northern Quebec. *4th TerraSAR-X Science Team Meeting*, Oberpfaffenhofen, Germany.

Parizzi, A. and Brcic, R., 2011. Adaptive InSAR Stack Multilooking Exploiting Amplitude Statistics: A Comparison Between Different Techniques and Practical Results, *IEEE Geoscience and Remote Sensing Letters*, 8(3), 441-445.

Rabus, B., Eppler, J., Sharma, J., and Busler, J., 2012. Tunnel monitoring with an advanced InSAR technique. *Proceedings of SPIE*, 8361, 83611F–83611F–10.

Short, N., Brisco, B., Couture, N., Pollard, W., Murnaghan, K., and Budkewitsch, P. 2011. A comparison of TerraSAR-X, RADARSAT-2 and ALOS-PALSAR interferometry for monitoring permafrost environments, case study from Herschel Island, Canada. *Remote Sensing of Environment*, 115(12), 3491-35.